β decay of ^{98}Ag: Evidence for the Gamow-Teller resonance near ^{100}Sn

Z. Hu,[1,4] L. Batist,[2] J. Agramunt,[3] A. Algora,[3] B. A. Brown,[4] D. Cano-Ott,[3] R. Collatz,[1] A. Gadea,[3] M. Gierlik,[5] M. Górska,[1] H. Grawe,[1] M. Hellström,[1] Z. Janas,[5] M. Karny,[5] R. Kirchner,[1] F. Moroz,[2] A. Płochocki,[5] M. Rejmund,[1] E. Roeckl,[1] B. Rubio,[3] M. Shibata,[1] J. Szerypo,[5] J. L. Tain,[3] and V. Wittmann[2]

[1]*Gesellschaft für Schwerionenforschung, D-64291 Darmstadt, Germany*

[2]*St. Petersburg Nuclear Physics Institute, RU-188-350 Gatchina, Russia*

[3]*Instituto de Física Corpuscular, Dr. Moliner 50, E-46100 Burjassot-Valencia, Spain*

[4]*Michigan State University, East Lansing, Michigan 48824*

[5]*Institute of Experimental Physics, University of Warsaw, PL-00681 Warsaw, Poland*

(Received 14 July 2000; published 20 November 2000)

In two complementary measurements, a cubelike array of six Euroball-Cluster germanium detectors and a total-absorption γ spectrometer were used to investigate the β decay of ^{98}Ag, a three-proton-hole and one-neutron-particle nucleus with respect to the ^{100}Sn core. The half-life and Q_{EC} value of the decay were determined to be 47.7(0.3) s and 8200(70) MeV, respectively. A total of 438 γ rays (414 new) was observed, and 173 levels (163 new) in ^{98}Pd have been identified. The Gamow-Teller (GT) β-decay strength distribution from the total-absorption γ spectroscopy reveals a large GT resonance around 6 MeV with a width of about 2 MeV. The hindrance factor for the total GT strength, summed from the ground state up to 7.8 MeV excitation energy in ^{98}Pd, amounts to 4.6(6) with reference to a shell-model calculation which yields good agreement with the shape of the experimental GT resonance.

PACS number(s): 23.40.−s, 23.50.+z, 27.60.+j, 29.30.−h

I. INTRODUCTION

The combination of two complementary experimental techniques, the high-resolution germanium-detector array (Cluster Cube) [1] and the low-resolution but high-efficiency total-absorption spectrometer (TAS) [2], has been demonstrated to be a powerful tool for investigating complex Gamow-Teller (GT) β decays of nuclei around the doubly magic nucleus ^{100}Sn [3] and around the semimagic nucleus ^{146}Gd [4]. This double strategy is especially useful for solving the problem of missing GT strength and for determining the GT hindrance factor. Following the ^{97}Ag experiment [3], we studied ^{98}Ag with the same experimental approach. In comparison to ^{97}Ag, ^{98}Ag is characterized by an additional neutron above the ^{100}Sn core, which resides predominantly in the $d_{5/2}$ orbital. This $d_{5/2}$ neutron and the three proton holes in the $g_{9/2}$ orbital determine the ground-state spin of ^{98}Ag. Shell-model calculations [5] and comparison to the ground-state spin of the isotone ^{96}Rh [6] favor a spin of 6^+ for the ground state of ^{98}Ag. On the basis of the extreme single-particle model, one expects the decay of ^{98}Ag to be dominated by a decay which mainly populates, after breaking a $\pi g_{9/2}^2$ pair, the four-quasiparticle states $[\pi g_{9/2}^{-1}\nu g_{7/2}]_{1^+}\pi g_{9/2}^{-1}\nu d_{5/2}$ in ^{98}Pd at excitation energies around 6 MeV [7]. It is tempting to try to experimentally probe this hypothesis, and to clarify whether the results obtained for ^{98}Ag by the two complementary methods are as close to each other as they were found to be for ^{97}Ag.

In this paper, we report on experimental data obtained for the ^{98}Ag decay by using the Cluster Cube and TAS array at the GSI on-line mass separator, equipped with a FEBIAD-B2C ion source [8]. ^{98}Ag was produced in fusion-evaporation reactions of a 50–80 particle-nA ^{40}Ca beam on a ^{61}Ni target, enriched to 86.4%. The $A=98$ beam delivered by the mass separator was implanted into the tape of a moving-tape collector, the resulting activity being transported to the center of the respective detector array in consecutive collection-measurement cycles. When presenting the experimental results in Secs. II and III, we refrain from giving details concerning the experimental techniques which have already been described in Refs. [1–3,9]. The notion E is used for the ^{98}Pd excitation energy, I_β for the β intensity including both EC and β^+ decay, I_{EC} and I_{β^+} for the intensities of each of these disintegration modes, and I_γ for the γ intensity including both EC and β^+ decay. In Sec. IV, we discuss the GT-strength distribution and the GT hindrance factor. Finally, a summary is given in Sec. V.

II. RESULTS FROM THE CLUSTER CUBE MEASUREMENT

A. Experimental technique

Beta-delayed γ rays of the ^{98}Ag decay were measured *with high energy resolution* by using the Cluster Cube which is an array of 42 germanium crystals [1]. The ^{40}Ca beam energy was 3.75A MeV, the thickness of the ^{61}Ni target amounted to 2.3 mg/cm^2. The ^{98}Ag beam intensity was estimated to be about 1100 atoms/s at a ^{40}Ca beam intensity of 65 particle×nA. The duration of the collection-measurement cycle was chosen to be 80 s. The total number of such cycles was 1680, corresponding to a total counting time of 38 h. More details on the experimental technique can be found in Refs. [1,3].

B. Gamma-ray singles and coincidence spectra

Figure 1 shows the γ-singles spectrum obtained from the list-mode data, which contains 1.8×10^8 events. As for ^{97}Ag

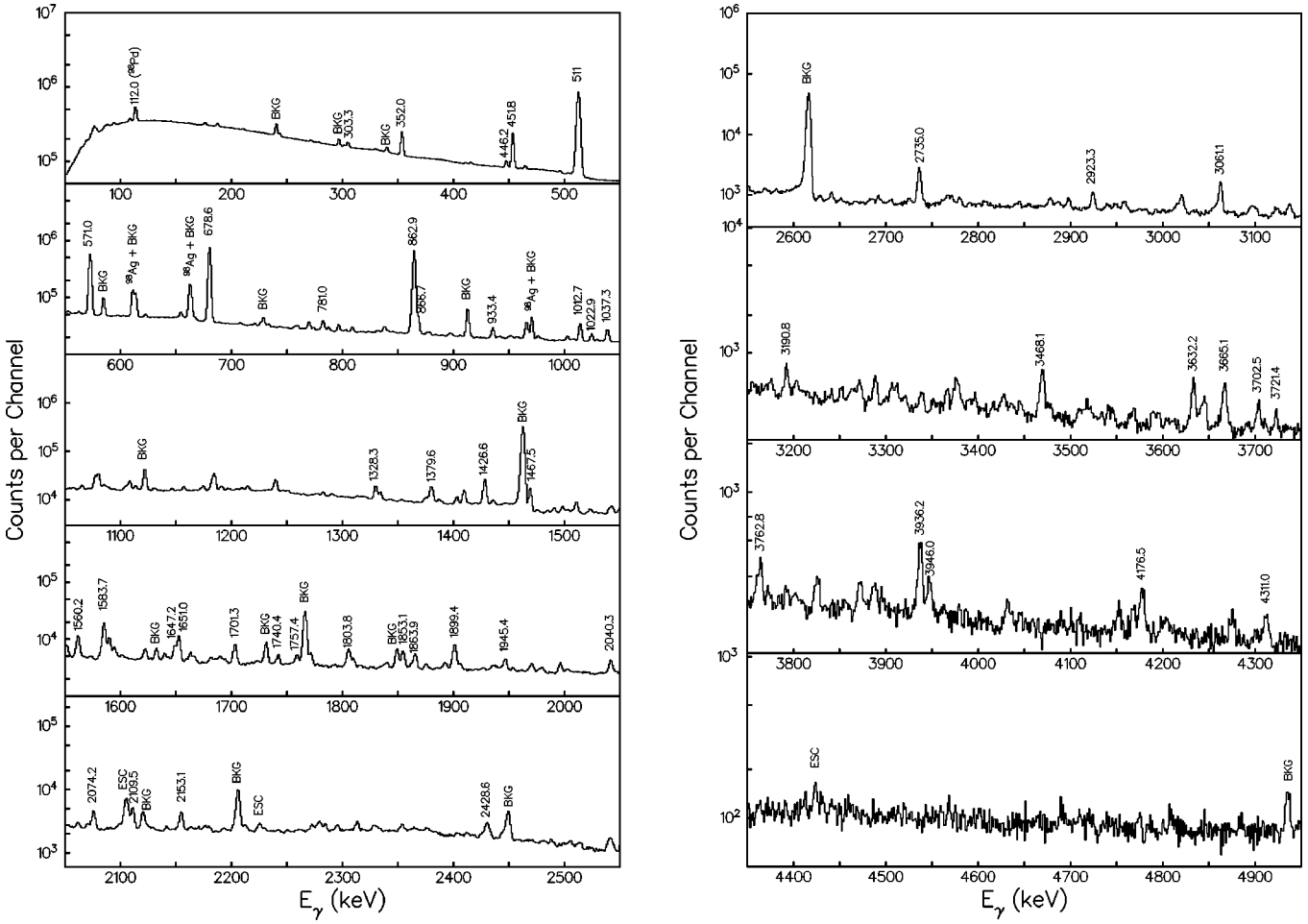

FIG. 1. Gamma-ray singles spectrum obtained by using the 42 capsules of the Cluster Cube for the measurement of mass-98 samples. See text for details.

[3], this spectrum is rather complex. Therefore, only a few representative γ lines from the ^{98}Ag decay are labeled in Fig. 1 by their energies in keV. In addition, contributions from isobaric contaminants (^{98}Pd), from room background (BKG) and from escape effects (ESC) are marked.

We obtained 3.8×10^{8} γ-γ coincidences from the Cluster Cube measurement by using the trigger described in Ref. [3]. In Fig. 2, a representative coincidence spectrum gated on the 862.8 keV γ-ray transition ($2^{+}\rightarrow0^{+}$) is shown. Again, because of the complexity of the spectrum, only a few representative γ rays from the ^{98}Ag decay are labeled by their energies in keV. The artificial peak (X) is related to a 1461 keV background γ ray (^{40}K as discussed in Ref. [3]).

The weakest γ ray identified in this work is shown in Fig. 3, which was determined to have an intensity value of 0.014% per β decay of ^{98}Ag. In the previous work using standard germanium detectors [10], the weakest γ-ray intensity was measured to be about 1%.

C. Half-life determination

17 γ lines were chosen for determining the half-life value of the ^{98}Ag decay, as shown in Table I. The resulting value of 47.7(0.3) s agrees with the previous result of 46.7(0.5) s [11].

D. Proposed decay scheme

1. Gamma transitions and levels in ^{98}Pd

The decay scheme for ^{98}Ag [12] obtained from this work includes 438 γ lines in total (414 new) and 173 excited states of ^{98}Pd (163 new). The methods used for placing γ transitions in the decay scheme and for determining their intensities are similar to those applied in our previous work [3]. The intensities of the γ transitions assigned to the ^{98}Pd level scheme were normalized to the total intensity of the transition from the first 2^{+} state to the ground state of ^{98}Pd. The average γ-ray multiplicity of 3.95(8), obtained from these data, will be discussed in Sec. III D.

2. Comparison with previous work

As mentioned in Sec. II D 1, the much higher detection sensitivity of the spectrometer used in this work compared to earlier investigations has allowed us to assign numerous new β-delayed γ rays to the ^{98}Ag decay, and to identify numerous new levels in ^{98}Pd. We are able to place in the ^{98}Ag $\rightarrow$^{98}Pd decay scheme all the γ transitions which, in the previous work [10], were assigned to this decay according to their half-life values but were not included in the decay scheme. In addition, we notice that our interpretation of as-

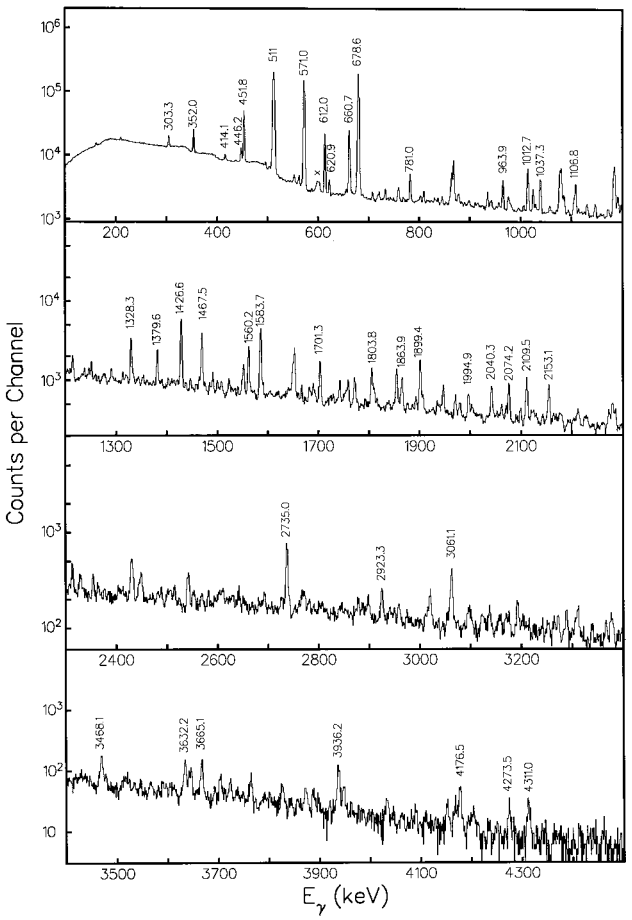

FIG. 2. Background-subtracted coincidence spectrum from the Cluster Cube data, gated on the 862.8 keV γ-ray transition. See text for details.

cribing the 352 keV γ line to the deexcitation of the 3076 keV level deviates from the proposals made by Kurcewicz *et al.* [10] and by Singh [11], who assigned this transition to originate from the 3441 keV and 3125 keV state, respectively.

E. Beta-intensity distribution

Under the assumption of a spin/parity assignment of 6^+ for the ground state of ^{98}Ag, mentioned in Sec. I, there are no allowed β transitions to the first 2^+ and 4^+ states in ^{98}Pd. The large (positive) I_β values, deduced for these levels from the γ-intensity balance, simply indicate that the high-resolution method has missed a sizable amount of γ intensity feeding these states. We shall discuss this problem further in Sec. III E.

III. RESULTS FROM THE TAS MEASUREMENT IN COMPARISON WITH CLUSTER CUBE DATA

A. TAS measurements

The TAS consists of a large NaI(Tl) crystal with a cylindrical well closed by an additional NaI(Tl) detector. The inserted radioactive sample is viewed by a pair of silicon detectors as well as by a germanium x-ray detector. The

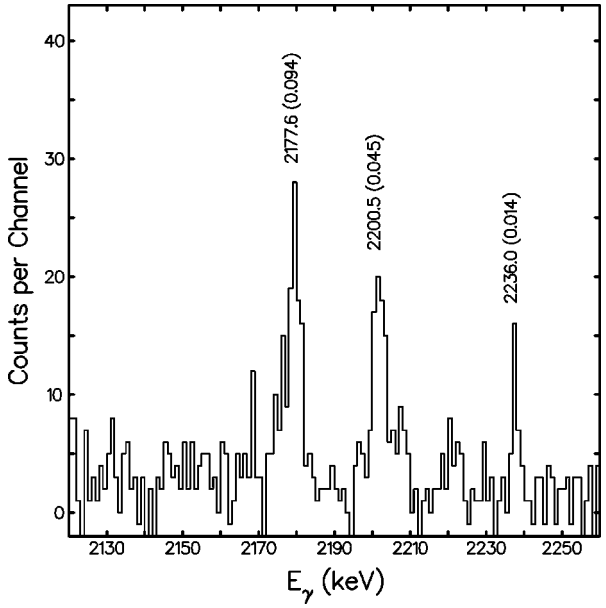

FIG. 3. Part of the background-subtracted coincidence spectrum from the Cluster Cube data, gated on the 1651.0 keV γ-ray transition, showing the 2236.0 keV γ-ray transition which is the weakest γ line from the ^{98}Ag decay identified in this work. The γ-ray intensity values in percent per β decay of ^{98}Ag are given within brackets following the transition energies in keV. Note that the 2177.6 keV γ line is in coincidence with a 1647.2 keV γ line and thus appears under the 1651.0 keV gate condition.

technique of using TAS for β-decay measurements has been described earlier [2,3,9], and will therefore only be briefly reviewed here. In contrast to the Cluster Cube measurement, the TAS data were taken by using the ''bunched'' mode of the ion source [13] in order to suppress the isobaric contami-

TABLE I. Gamma-ray transitions used for the determination of the half-life of ^{98}Ag.

E_γ (MeV)	$T_{1/2}$ (s)
303.3	43(7)
451.8	49(3)
571.0	48.0(6)
678.5	47.3(5)
862.8	49.1(6)
1012.7	39(3)
1022.9	42(9)
1037.3	55(7)
1183.0	48.5(9)
1426.6	46.8(13)
1560.2	51(10)
1651.0	49(6)
1701.3	40(6)
1899.4	50(7)
2074.2	30(6)
2735.0	30(3)
3061.1	40(10)
average	47.7(3)

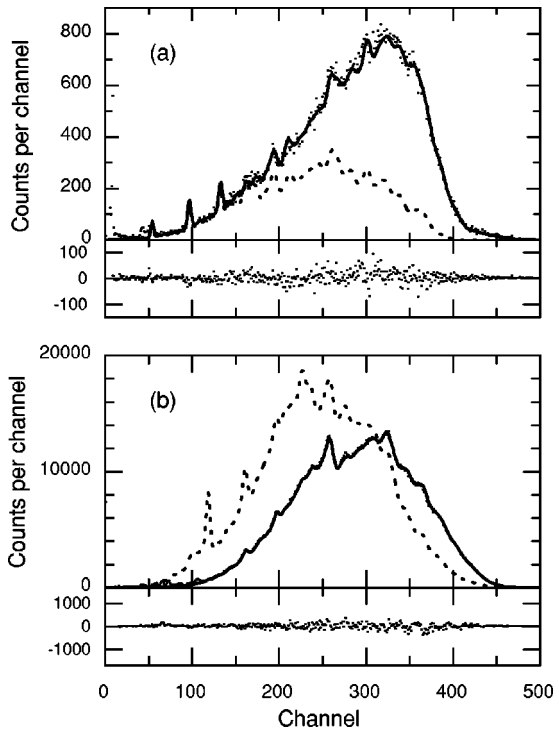

FIG. 4. TAS spectrum for the EC (a) and β^+ (b) decay of ^{98}Ag from experiment (filled squares), from simulations based on the least-square fit (solid line), and from simulations obtained by using the β-intensity distribution due to the Cluster Cube data (dotted line). The latter data set was adapted to the TAS energy resolution by a smoothing procedure. The difference between the experimental data and least-square fit is displayed in a separate section of each panel. The small peaks below channel 50 in panel (a) and below channel 110 in panel (b) stem from ^{98}Pd and ^{98}Rh contributions which have not been included in the simulations.

nation. The ^{40}Ca beam energy was 3.86*A* MeV, and the thickness of the ^{61}Ni target amounted to 2.5 mg/cm^2. A total of 1680 collection-measurement cycles, each of a duration of 96 s, were devoted to the TAS experiment on ^{98}Ag, corresponding to a total counting time of 23 h. After each third cycle, the room background was measured in TAS during 96 s, while the $A=98$ beam was directed to another tape collector for monitoring the source composition by means of a standard germanium detector. In order to identify and control the contribution of the contaminants, TAS spectra of ^{98}Pd and ^{98}Rh were recorded in separate measurements performed with longer collection-measurement cycles.

B. Experimental TAS spectra and determination of EC/total ratio

By demanding coincidences of TAS signals with palladium x rays registered in the germanium detector, or with positrons recorded in the silicon detectors, we distinguish between events related to EC or β^+ decay of ^{98}Ag. The resulting spectra ''EC-TAS'' and ''β^+-TAS,'' which are displayed in Fig. 4, have to be distinguished from the ''TAS singles spectrum'' which has been accumulated without any coincidence condition. The main restriction in statistics of the EC-TAS spectrum stems from the small efficiency of the germanium crystal used for x-ray detection: Out of a total of 1.2×10^6 ^{98}Ag decays recorded in TAS, only about 1.4×10^4 events were selected as being due to the EC decay of this isotope.

At first we shall discuss the general properties of the experimental TAS spectra, and shall in particular inspect their purity which plays an important role in the subsequent data evaluation.

The TAS singles spectrum is seriously distorted by contributions from the room background and from the isobaric contaminants ^{98}Pd and ^{98}Rh, which are mostly produced as daughter and granddaughter products of ^{98}Ag. On the basis of the EC-TAS and β^+-TAS data, the number of ^{98}Pd events in the total TAS spectrum was estimated to be of the order of 10% compared to those assigned to ^{98}Ag.

The EC-TAS spectrum is free of contributions from room background, but contains a small admixture of ^{98}Pd decay events. This contamination is due to the high-energy tail of the rhodium K x-ray line, which extends into the palladium K x-ray gate chosen for generating the EC-TAS spectrum. The contribution from ^{98}Pd decay to the EC-TAS spectrum lies below the energy of the first excited state of ^{98}Pd, populated in EC decay of ^{98}Ag, and hence represents only a negligible distortion of the dominating ^{98}Ag part.

The β^+-TAS spectrum, displayed in Fig. 4, is dominated by ^{98}Ag activity but contains also ^{98}Pd and ^{98}Rh events. This contamination has been taken into account in the following determination of EC/total ratios, even though it is weak, occurs at low energy, and has hence no major influence on the results. Due to registration of γ rays in the silicon detectors, the β^+ TAS-spectrum actually includes some EC events. Using experimental data, we estimated that the efficiency of the silicon detectors for γ rays *following EC decay* of ^{98}Ag is of the order of 10% of their efficiency for positrons.

We turn now to the determination of the ratio between EC and (EC+β^+) intensities for the decay of ^{98}Ag, integrated over the entire range of the TAS spectra. This quantity was found to be EC/total=0.360(25) by subtracting the contributions due to room background and isobaric contaminants from the TAS singles spectrum, and decomposing it then into components being proportional to the EC-TAS and β^+-TAS spectra, as described in [3]. The determination of this value is not completely independent of the underlying ^{98}Ag decay scheme, as we performed corrections for summing effects occurring in the germanium detector and for the distortion of the β^+-TAS spectrum related to the registration of EC-delayed γ rays in the silicon detectors. These two effects yield the main contribution to the uncertainty of the EC/total value.

The β intensity distribution derived from the Cluster Cube data would yield EC/total values of only 0.13 or 0.16, if the Q_{EC} value of ^{98}Ag is assumed to be 8230 keV [14] or 8420 keV [15] (see also the discussion in Sec. III C). The discrepancy between this result and that deduced from the TAS data indicates again the incompleteness of the decay scheme obtained from the Cluster Cube measurement. This feature is confirmed by comparing the EC-TAS and the β^+-TAS spec-

tra to those obtained by a simulation based on the Cluster Cube data (see Fig. 4). The simulations were performed by using the code GEANT3 with TAS parameters described in [16]. While the discrepancy between the experimental and the simulated spectra was small in the case of ^{97}Ag [3], it is considerably larger for ^{98}Ag, indicating in particular that the Cluster Cube measurement has missed many γ transitions from *higher-lying* ^{98}Pd states.

C. Deconvolution of TAS spectra and determination of the Q_{EC} value

In order to obtain the β-intensity distribution for ^{98}Ag, we simulated a set of TAS spectra corresponding to the population of selected levels, and fitted them to the experimental TAS spectra by a least squares method, with the β intensities of these levels being variable parameters. This method involves of course the Q_{EC} value which, as will be shown below, can be determined in this way on the basis of experimental data.

The simulations were performed by using the code GEANT3, with the initial assumption concerning the level scheme and $I_\gamma(E)$ distribution being derived from the Cluster Cube data. The unfolding procedure applied here differs from the ''peel-off'' method that we used in our previous work [3]. The modification was realized with the aim of making a least-squares method available that allows one to take additional physical conditions into account in an easy and controlled way. The method chosen enables one to (i) simultaneously fit both EC-TAS and β^+-TAS spectra by using one and the same β-intensity distribution, and (ii) additionally fulfill the condition that the resulting $I_\gamma(E)$ distribution should agree with that derived from the Cluster Cube data for low-lying ^{98}Pd levels. In addition to the latter data set, we included a number of ''pseudo'' levels [9] which were placed in consecutive 100 keV intervals above ^{98}Pd excitation energies of 4 MeV. We did not try to adjust the position of the pseudo levels to the structure of the experimental EC-TAS and β^+-TAS spectra, as the simulation based on the Cluster Cube data apparently exhausts all pronounced peaks observed experimentally (see Fig. 4). Therefore, the pseudo levels serve to describe the part of the β-intensity distribution that is scattered over a great number of real levels.

The response function R_i for the ith pseudo level was calculated as $R_i = \Sigma b_{i,k} r_{i,k} R_k$, where $r_{i,k}$ is the response function for a γ ray with an energy $(E_i - E_k)$, and R_k the response function for the kth real level. R_k is completely defined by the decay scheme obtained from the Cluster Cube data, but does not depend on the β intensities determined in the latter analysis. We assumed that the branching ratios $b_{i,k}$ for the γ transitions from a pseudo level to the set of low-lying levels obey a statistical pattern, i.e., $b_{i,k} \propto a_k \cdot (E_i - E_k)^3$, the coefficients a_k being parameters in the fitting procedure. In order to reduce the number of such parameters, closely spaced and weakly populated levels within this set were bunched into groups. We started with 35 different values for the β intensities $I_{\beta,k}$ of the low-lying levels, the same number of parameter for γ-branching ratios a_k, and 40 parameters for the β intensities of pseudolevels. During the least-squares procedure, some of the a_k values showed the persistent trend to be negative and hence were set to zero. The fit yielded also negative values for some of the parameters related to the β-intensity distribution. However, the corresponding intensity remained small, i.e., within the statistical uncertainty limits of the experimental data.

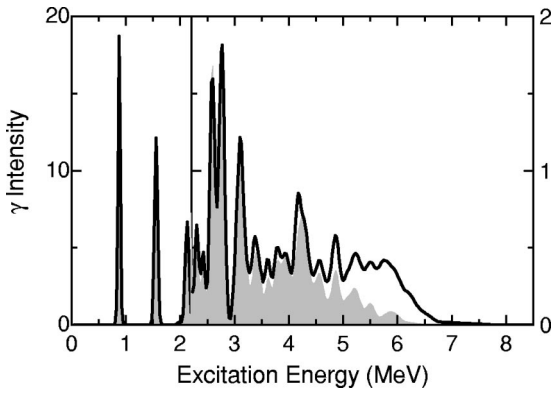

FIG. 5. Gamma intensity for the β decay of ^{98}Ag as a function of ^{98}Pd excitation energy, derived from TAS data (solid line) and from the Cluster Cube measurement (shaded area). The γ intensity is defined as the number of quanta emitted per β decay, integrated over an excitation-energy interval of 1 MeV. The ordinate scale is reduced by a factor of 10 for excitation energies above 2.2 MeV.

The statistics in the β^+-TAS spectrum was about 15 times better than that in the EC-TAS one. Therefore, in order to avoid complete suppression of the latter during the joint least-squares procedure mentioned above, we applied a weight factor of 0.1 to the β^+-TAS spectrum. We then started fitting both the EC-TAS and the β^+-TAS spectrum for an initial value of Q_{EC}. The resulting β-intensity distribution allowed us to determine an (integrated) EC/total ratio. We then repeated the procedure by using other Q_{EC} values in an attempt to reproduce the experimental EC/total value of 0.360(25), mentioned in Sec. III B, and got a Q_{EC} value of 8200(60) keV.

The final result for the simulated EC-TAS and β^+-TAS spectrum shows good agreement with the corresponding experimental spectra (see Fig. 4), the χ^2 values for one degree of freedom being 1.3 and 2.0, respectively. The latter result indicates sizable nonstatistical contributions. The distributions of I_γ and I_β, obtained from the least-squares analyses of the EC-TAS and β^+-TAS spectra, are displayed in Figs. 5 and 6 together with the corresponding data obtained from the Cluster Cube measurement. The statistical uncertainties of the I_β values are rather small in the region of the distribution where the main part of the intensity is located, and amount to about 4% for ^{98}Pd excitation energies above 4 MeV. A detailed inspection of the least-squares fits revealed that the I_β uncertainties, including nonstatistical contributions, are about 7% for $E \leqslant 6.3$ MeV.

By using a *fixed* set of a_k, we performed an additional least-squares analysis *separately* for the EC-TAS and β^+-TAS spectra. The resulting χ^2 values of 1.15 and 1.7, respectively, are considerably smaller than those obtained from the *joint* analysis. This indicates some inconsistency

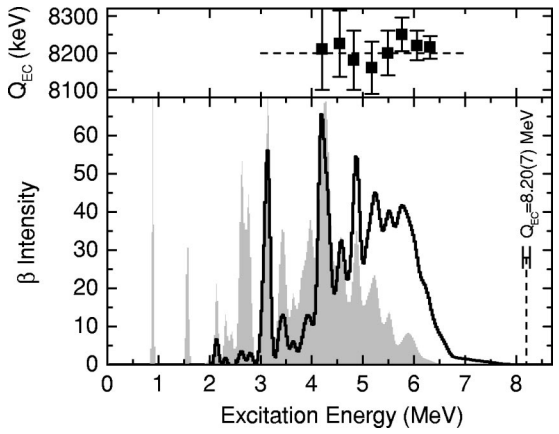

FIG. 6. Lower panel: Beta intensity for the decay of ^{98}Ag as a function of ^{98}Pd excitation energy, obtained from the deconvolution of the experimental TAS spectra (solid line) and from the Cluster Cube data (shaded area). The β intensity is defined as the (β^+ + EC) feeding in percent per decay, integrated over an excitation-energy interval of 1 MeV. Upper panel: Q_{EC} value derived from a joint least-squares analysis of the TAS data (horizontal dashed line), and Q_{EC} values determined on the basis of I_{EC}/I_{β^+} ratios for the different excitation-energy intervals (squares). The error bars stem from the uncertainties of the individual Q_{EC} values, which are mainly determined by the uncertainty of the integrated EC/total ratio.

between the EC-TAS and β^+-TAS data. On the one hand, the statistical I_{EC} uncertainties are larger than 100% for the low E values but decrease rapidly for $E \geqslant 4$ MeV. On the other hand, the I_{β^+} data derived from the β^+-TAS spectrum can be used up to $E \approx 6.3$ MeV. For such a high excitation energy, however, about 50% of the events in this spectrum are due to the registration of EC-delayed γ rays in the silicon detectors. Therefore, the interval $4.0 \leqslant E \leqslant 6.3$ MeV can be used for checking the consistency of the analysis. The result of this verification is presented in the upper panel of Fig. 6, which shows the E dependence of individually determined Q_{EC} values corresponding to individually determined ratios I_{EC}/I_{β^+}. In this calculation, we used statistical rate functions of beta decay [18], and normalized I_{EC} and I_{β^+} on the basis of the experimental EC/total value discussed in Sec. III B. The average over the individual Q_{EC} values, calculated in such a way for the different energy bins, is practically the same as that obtained from the above-mentioned joint least-squares procedure. Including the uncertainties of the individual Q_{EC} values as well as those of the related E values, we obtain $Q_{EC} = 8200(75)$ keV.

Finally, we accept a Q_{EC} value of 8200(70) keV for ^{98}Ag as a joint result from both methods presented in this section. This result agrees with that given in the 1983 Atomic Mass Table [8230(300) keV] [14], and also with the somewhat higher value included in its 1993 version [8420(150) keV] [15]. In the latter case, the Q_{EC} value was based on the β-end-point energy of 6880(150) keV derived by Verplancke *et al.* [17] from a singles positron measurement, and on the corresponding level energy of 1542 keV [11]. However, these authors indicated [17] that their β-end-point energy has to be considered as a lower limit as the major β^+/EC feeding may go to unknown high-lying ^{98}Pd states. This supposition actually turned out to be true: Instead of a strong β feeding of 19% [11] for the 1542 keV level, assumed in deriving the Q_{EC} value of 8420(150) keV [15], the TAS data presented in this work indicate an upper limit of 0.15% for this feeding (see Sec. III E). These considerations shed some doubts on the reliability of the Q_{EC} value for ^{98}Ag given in Ref. [15], and also show the general problem involved in deriving β-decay Q values from β-end-point energies determined of far-unstable nuclei without sufficient knowledge of the decay scheme.

D. Gamma-intensity distributions

Figure 5 shows the $I_\gamma(E)$ distribution derived from the TAS data, together with the corresponding spectrum deduced from the Cluster Cube measurements. Similar to the results obtained for the ^{97}Ag decay, there is relatively good agreement between both data sets up to $E = 4$ MeV. The difference of approximately 0.2 quanta/decay for this energy range can be explained by the uncertainties of the fitting procedure applied to the TAS results. For $E \geqslant 4.5$ MeV the $I_\gamma(E)$ distribution determined from the TAS experiment systematically lies above that based on the Cluster Cube data. The excess γ intensity of 0.44 quanta/decay for this energy range is considerable larger than the value of 0.09 quanta/decay, obtained for the case of ^{97}Ag [3]. That the Cluster Cube has missed such a large fraction of the I_γ distribution of ^{98}Ag is evidently related to the fact that the β strength of this decay moves to higher E values and is more fragmented compared to ^{97}Ag (see Sec. IV). A close inspection of the coincidence spectrum from the Cluster Cube data, gated on the lowest lying γ-ray transition in ^{98}Pd (see Fig. 2), with the corresponding ^{97}Ag data (see Fig. 2 of [3]) shows that the level of unresolved continuous ''background'' underneath the photopeaks is considerable higher for ^{98}Ag. This indicates that there is evidently a sizeable contribution from unresolved (high-energy) γ rays (see also Sec. III E).

The average γ-ray multiplicity, deduced from the TAS data, amounts to 4.55(15), compared to a value of 3.95(8) obtained from the Cluster Cube measurement (see Sec. II D 1). As the γ transitions deexciting the first three excited ^{98}Pd levels represent an average multiplicity of 2.6, about 25% of the high-lying (fragmented) $I_\gamma(E)$ distribution has evidently been missed by the Cluster Cube experiment.

E. β feeding distribution

The $I_\beta(E)$ distribution of ^{98}Ag obtained by unfolding the EC-TAS and β^+-TAS spectra is presented in Fig. 6 in comparison with the corresponding Cluster Cube result. The TAS data do not give evidence for a strong population of ^{98}Pd levels below $E = 2.9$ MeV. As can be seen from Fig. 6, in this energy region only the level at 2100 keV is fed with an appreciable intensity of $I_\beta = 0.60(30)\%$, while the population of neighboring states is smaller, e.g., $I_\beta \leqslant 0.15\%$ for the levels at 863 and 1540 keV, and amounts in total to less than 1%. The results from the TAS and Cluster Cube measurements agree for the ^{98}Pd level at 3125 keV, which was sup-

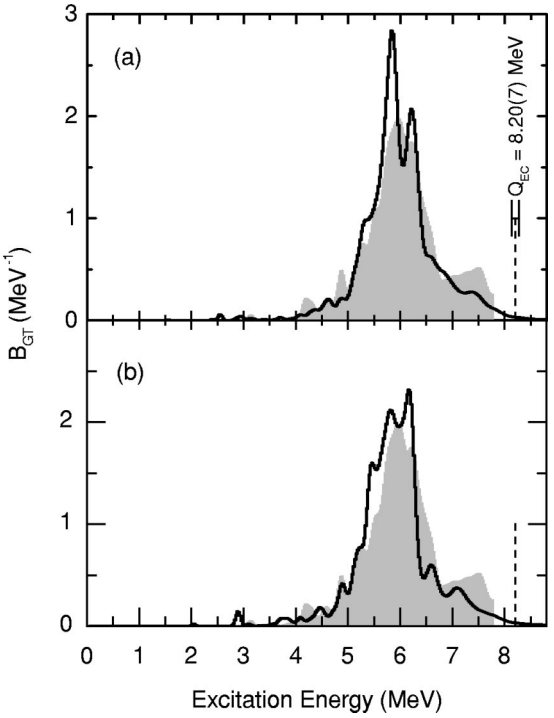

FIG. 7. GT-strength distributions for the decay of ^{98}Ag obtained from the TAS measurement (shaded area) and from the SNC shell-model calculation (solid line) assuming the ^{98}Ag ground-state spin of 5^+ (a) and 6^+ (b). The theoretical GT strength has been reduced by a hindrance factor of 4.6.

posed in the previous works [10,19] to have a tentative spin assignment of 6^+. Furthermore, they agree with respect to their gross structure for $E \geqslant 4$ MeV, where the main part of the $I_\beta(E)$ distribution is located. It is evident from a comparison of Figs. 5 and 6 that the Cluster Cube measurement was mainly sensitive to γ rays emitted from those ^{98}Pd levels that are strongly populated in ^{98}Ag decay. Nevertheless, a detailed analysis of the $I_\beta(E)$ distribution shows that about 30% of the intensity, that has been missed by the Cluster Cube, has to be assigned to ^{98}Pd levels *near* the strongly populated ones.

F. Evaluation of Gamow-Teller strength function

We determined the GT strength function B_{GT} for the ^{98}Ag decay by using the expression $B_{GT}=3860\, I_\beta / f\, t$, where $f = f_{EC} + f_{\beta^+}$ is the statistical rate function for EC and β^+ decay, which depends on the value of $(Q_{EC}\text{-}E)$ [18], t is the half-life which for ^{98}Ag has previously been determined to be 47.7(0.3) s (see Sec. II C), and I_β is normalized to $\Sigma I_\beta = 1$. We assumed a Q_{EC} value of 8200(70) keV as determined in this work (see Sec. III C), and used the I_β results from the TAS analysis (see Sec. III E). The resulting B_{GT} is shown in Fig. 7. The B_{GT} uncertainties do not exceed 10% for $E \leqslant 7.5$ MeV. However, they dramatically increase for higher E values, and lead to completely unreliable B_{GT} values for $E \geqslant 7.7$ MeV. The integrated B_{GT} value amounts to 2.7(4) for $E \leqslant 7.7$ MeV, the uncertainty being dominated by contributions from the integrated EC/total ratio and the Q_{EC} value.

IV. GAMOW-TELLER STRENGTH DISTRIBUTION AND ITS HINDRANCE

As mentioned already in Sec. I, the extreme single-particle model predicts the ^{98}Ag decay to be dominated by transitions to four quasiparticle states in ^{98}Pd, which lie at excitation energies of about 6 MeV. The position of the experimental GT resonance qualitatively confirms this expectation. A more detailed analysis of the GT strength distribution was performed in the same manner as for the ^{97}Ag decay [3]. The shell model results were obtained with the SNB basis. The SNB basis for ^{98}Ag (^{98}Pd) consists of three (four) proton holes in the $p_{1/2}$ and $g_{9/2}$ orbitals and one (two) neutrons in the $g_{7/2}$, $d_{5/2}$, $d_{3/2}$, $s_{1/2}$, and $h_{11/2}$ orbitals. As has already been discussed for the case of the ^{97}Ag decay [3], the centroid of the GT distribution, obtained with the original SNB Hamiltonian, could be brought into better agreement with experiment by a small increase of the normalization of the proton-neutron G matrix from $N_{pn}=0.70$ (SNB) to $N_{pn}=0.77$ (SNC). In order to be consistent with the ^{97}Ag analysis, in this paper we used the SNC Hamiltonian. With the SNC (and SNB) Hamiltonian the spin/parity of the ^{98}Ag ground-state could be 5^+ and 6^+, both levels being less than 100 keV apart. Since an experimental spin-parity assignment is not available, we calculated the GT distributions for both cases. As can be seen from Fig. 7, the GT distribution obtained for the two choices of ^{98}Ag ground-state spin-parity are similar, and both are in good agreement with the centroid and the width of the experimental GT resonance.

In the extreme single-particle model, the ^{98}Ag decay, with three holes in $g_{9/2}$ orbit and one particle in $d_{5/2}$ orbit, has the same total GT strength as the ^{97}Ag decay, namely 12.45. For both 5^+ and 6^+ ground-state configurations, the $d_{5/2}$ occupancy in ^{98}Ag is about 90%, and the SNC calculation yields a total GT strength of 12.44. When comparing with the experimental strength of 2.7(4), we obtain a hindrance factor of 4.6(6). Within the respective experimental uncertainties, this result agrees within that of 4.3(6) obtained for the ^{97}Ag decay [3].

The SNC Hamiltonian gives a GT β-decay half-life of 9.1 s (5^+) and 7.8 s (6^+), where we use the experimental Q_{EC} value of 8.20 MeV. For a comparison with the experimental half-life, a hindrance factor of 5.2 (5^+) and 6.1 (6^+) would be obtained. It is not surprising that these results deviate from the hindrance factor of 4.6(6) extracted from a comparison of total GT strengths. Such discrepancies occur as the hindrance deduced from the half-life is a measure of the β *intensity* while the hindrance determined from the *strength* may be different due to the strongly energy-dependent phase-space factor. It is also clear that the determination of the GT hindrance factor based on a comparison of experimental and theoretical *strength* distribution is the more valuable if not the only possible way of discussing GT hindrance.

V. SUMMARY

This work is a continuation of applying two powerful complementary set ups, i.e., Cluster Cube and TAS, to investigate the β decay of very neutron-deficient isotopes near

^{100}Sn. Despite of the observation of numerous γ lines (438) for the ^{98}Ag decay and the identification of many excited states (173) in ^{98}Pd, the Cluster Cube was unable to fully register the complex β decay of ^{98}Ag. If normalized to the result obtained by TAS, the Cluster Cube data failed to observe 12.4% of the total γ intensity. This is about a factor of 4 times more than in case of the ^{97}Ag-decay study [3]. The common feature in the study of these two silver isotopes is that almost all the unobserved γ intensity lies above 4 MeV excitation energy of the daughter nuclei. The reason why the high-resolution measurement missed more γ intensity in the case ^{98}Ag decay is evidently related to the fact that its β decay populates four quasiparticle states in ^{98}Pd, whose excitation energies and level density are higher than those of three quasiparticle states populated in the ^{97}Ag decay. With the same detection sensitivity of the high-resolution array, it is obvious that the investigation of the more complex β decay of ^{98}Ag is more difficult. In view of the incompleteness of detecting the γ intensities by means of the Cluster Cube, we were unable to derive a correct β-intensity distribution by using the traditional γ-intensity balance, and to calculate the GT strength from these data. This problem might be solved by a future analysis of the continuous part of these high-resolution spectra. However, the Cluster Cube measurement is still useful as the resulting detailed decay scheme forms the basis for de-convoluting TAS spectra.

The high-efficiency device TAS has allowed us to identify a dominant GT resonance occurring in the decay of ^{98}Ag. The resonance centers at ^{98}Pd excitation energies of about 6 MeV and has a width of about 2 MeV, which is in qualitative agreement with expectations based on the extreme single-particle model. A shell-model calculation within the restricted SNB basis reproduces the excitation energy and overall shape of the GT-strength distribution despite the discrepancy in the summed GT strength. The GT hindrance factor, obtained by comparing the SNB prediction to the TAS data, amounts to 4.6(6), which is in agreement with the value of 4.3(6) deduced for the ^{97}Ag decay. A more detailed discussion of the mass dependency of the GT hindrance factor for nuclei near ^{100}Sn will be given in a forthcoming paper.

For the β decay of the *odd-even* nucleus ^{97}Ag, the data obtained with the high-resolution Cluster Cube match closely the TAS-based GT-strength distributions, whereas in the case of the *odd-odd* nucleus ^{98}Ag the larger decay energy and the feeding of highly-excited four-quasiparticle structures in the daughter nucleus ^{98}Pd made the Cluster Cube study less reliable with respect to the GT-strength properties. In view of this discrepancy, it would clearly be interesting to apply the TAS technique to previously studied (and claimed to be simple) decays of *even-even* nuclei near ^{100}Sn. In fact, a TAS measurement of ^{98}Cd has been initiated.

Last not least, TAS allows one also to investigate other properties than the β-intensity distribution. This may be illustrated by two examples. First, weak isomeric γ and conversion electron transitions could be searched for by using the Ge and Si detectors, respectively, with an anticoincidence condition derived from the NaI(Tl) detectors for suppression of β-delayed and room-background γ rays. Second, measurements of β-delayed particles in coincidence with γ and x rays could be performed. For this purpose, one would use the Si detector (or a ΔE-E telescope), facing the implantation side of the tape, for recording charged particle, and the NaI(Tl) and Ge detectors for measuring γ and x rays, respectively.

ACKNOWLEDGMENTS

This work was supported in part by the European Community under Contract No. ERBFMGECT950083, by the German BMBF under the scientific-technical collaboration projects POL 99/009 and RUS 98/672, by the Polish Committee of Scientific Research under Grant No. KBN 2 P03B 086 17, by the Russian Fund for Basic Research and the Deutsche Forschungsgemeinschaft under Contract No. 436 RUS113/201/0(R), and by the C.I.C.Y.T. (Spain) under project AEN96-1662, and by the U.S. National Science Foundation under Grants No. PHY-9605207 and No. PHY-0070911. The authors would like to thank the German Euroball Collaboration for making the Euroball Cluster detectors available for this experiment. These detectors were supported by the German BMBF, the KFA Jülich, the GSI Darmstadt, and the MPI-K Heidelberg. B.A.B. wishes to thank the Alexander von Humboldt Foundation for support. M. Górska and M. Karny wish to thank the Foundation for Polish Science for support.

[1] Z. Hu, R. Collatz, H. Grawe, and E. Roeckl, Nucl. Instrum. Methods Phys. Res. A **419**, 121 (1998).

[2] M. Karny, J.M. Nitschke, L.F. Archambault, K. Burkard, D. Cano-Ott, M. Hellström, W. Hüller, R. Kirchner, S. Lewandowski, E. Roeckl, and A. Sulik, Nucl. Instrum. Methods Phys. Res. B **126**, 411 (1997).

[3] Z. Hu, L. Batist, J. Algora, B.A. Brown, D. Cano-Ott, R. Collatz, A. Gadea, M. Gierlik, M. Górska, H. Grawe, M. Hellström, Z. Janas, M. Karny, R. Kirchner, F. Moroz, A. Płochocki, M. Rejmund, E. Roeckl, B. Rubio, M. Shibata, J. Szerypo, J.L. Tain, and V. Wittmann, Phys. Rev. C **60**, 024315 (1999).

[4] J. Agramunt, A. Algora, D. Cano-Ott, A. Gadea, B. Rubio, J.L. Tain, M. Gierlik, M. Karny, Z. Janas, A. Płochocki, K. Rykaczewski, J. Szerypo, R. Collatz, J. Gerl, M. Górska, H. Grawe, M. Hellström, Z. Hu, R. Kirchner, M. Rejmund, E. Roeckl, M. Shibata, L. Batist, F. Moroz, V. Wittmann, and P. Kleinheinz, in *Proceedings of the International Symposium on New Facet of Spin Giant Resonance in Nuclei*, Tokyo, 1997, edited by H. Sakai, H. Okamura, and T. Wakasa (World Scientific, Singapore, 1998), p. 150.

[5] R. Schubart, H. Grawe, J. Heese, H. Kluge, K. H. Maier, and M. Schramm, Z. Phys. A **462**, 373 (1995).

[6] W.F. Piel, Jr., D.B. Fossan, R. Ma, E.S. Paul, N. Xu, and J.B.

Mcgrory, Phys. Rev. C **41**, 1223 (1990).
[7] B.A. Brown and K. Rykaczewski, Phys. Rev. C **50**, 2270 (1994).
[8] R. Kirchner, D. Marx, O. Klepper, V.T. Koslowski, T. Kühl, P.O. Larsson, E. Roeckl, K. Rykaczewski, and D. Schardt, Nucl. Instrum. Methods Phys. Res. A **234**, 224 (1985).
[9] M. Karny, L. Batist, B.A. Brown, D. Cano-Ott, R. Collatz, A. Gadea, R. Grzywacz, A. Guglielmetti, M. Hellström, Z. Hu, Z. Janas, R. Kirchner, F. Moroz, A. Piechaczek, A. Płochocki, E. Roeckl, B. Rubio, K. Rykaczewski, M. Shibata, J. Szerypo, J. L. Tain, V. Wittmann, and A. Wöhr, Nucl. Phys. **A640**, 3 (1998).
[10] W. Kurcewicz, E.F. Zganjar, R. Kirchner, O. Klepper, E. Roeckl, P. Komninos, E. Nolte, D. Schardt, and P. Tidemand-Petersson, Z. Phys. A **308**, 21 (1982).
[11] B. Singh, Nucl. Data Sheets **84**, 565 (1998).
[12] Z. Hu (unpublished).
[13] R. Kirchner, Nucl. Instrum. Methods Phys. Res. B **26**, 204 (1987).
[14] A.H. Wapstra and G. Audi, Nucl. Phys. **A432**, 1 (1983).
[15] G. Audi and A.H. Wapstra, Nucl. Phys. **A565**, 1 (1993).
[16] D. Cano-Ott, J.L. Tain, A. Gadea, B. Rubio, L. Batist, M. Karny, and E. Roeckl, Nucl. Instrum. Methods Phys. Res. A **430**, 333 (1999).
[17] J. Verplanke, D. Vandeplassche, M. Huyse, K. Cornelis, and G. Lhersonneau, in *Proceedings of the 6th International Conference on Atomic Masses*, East Lansing, 1979, edited by J.A. Nolen, Jr., and W. Benenson (Plenum, New York, 1980), p. 431.
[18] N.B. Gove and M.J. Martin, Nucl. Data Tables **10**, 205 (1971).
[19] M. Huyse, K. Cornelis, G. Dumont, G. Lhersonneau, J. Verplancke, and W.B. Walters, Z. Phys. A **288**, 107 (1978).